HIGH EFFICIENCY SOLAR POWER AND BATTERY BASED HYBRID MICRO GRID USING UNIFIED CONTROL SCHEME

Author name: Mr. B.Satheeshprabu. ME, Assistant professor EEE department, VSB Engineering college ,Karur
Co-author: Chenniyappan.p ,Saranraj.M , Sivaraja.M , Velusamy.G , Electrical and electronics engineering
VSB Engineering college, karur. E-mail ID: satheeshprabu1987@gmail.com, E-mail Id: enniyappan345@gmail.com

***Abstract*—Battery storage is usually employed in Photovoltaic (PV) system to mitigate the power fluctuations due to the characteristics of PV panels and solar irradiance. Control schemes for PV-battery systems must be able to stabilize the bus voltages as well as to control the power flows flexibly. This paper proposes a comprehensive control and power management system (CAPMS) for PV-battery-based hybrid microgrids with both AC and DC buses, for both grid-connected and islanded modes. The proposed CAPMS is successful in regulating the DC and AC bus voltages and frequency stably, controlling the voltage and power of each unit flexibly, and balancing the power flows in the systems automatically under different operating circumstances, regardless of disturbances from switching operating modes, fluctuations of irradiance and temperature, and change of loads. Both simulation and experimental case studies are carried out to verify the performance of the proposed method.**

***Index Terms*—Solar PV System, Battery, Control and Power Management System, Distributed Energy Resource, Microgrid, Power Electronics, dSPACE.**

I. INTRODUCTION

CONTINUALLY increasing demand for energy and concerns of environmental deterioration have been spurring electric power experts to find sustainable methods of power generation. Distributed generations (DG) in the form of renewable resources, such as solar energy, are believed to provide an effective solution to reduce the dependency on conventional power generation and to enhance the reliability and quality of power systems [1]. Photovoltaic (PV) power systems have become one of the most promising renewable generation technologies because of their attractive characteristics such as abundance of solar and clean energy. Rapid PV technology development and declining installation costs are also stimulating the increasing deployment of PV in power systems. However, due to the nature of solar energy and PV panels, instantaneous power output of a PV system depends largely on its operating environment, such as solar irradiance and surrounding temperature, resulting in constant fluctuations in the output power [2], [3]. Therefore, to maintain a reliable output power, battery storage systems are usually integrated with PV systems to address the variability issue.

A typical configuration of PV-battery system is illustrated in Fig. 1, which is a hybrid microgrid system consisting of a PV array that contains a number of PV panels, battery bank for power storage, and a centralized bidirectional inverter that interfaces the DC to AC power system [4], [5]. A unidirectional DC/DC converter is installed to control the power of PV arrays, while the battery bank is charged/discharged by controlling a bidirectional converter that bridges the battery and the DC bus. DC loads are supplied through direct connection to the DC bus and AC loads and the point of common coupling (PCC) is located on the AC side. Before connecting to the utility grid, a transformer is employed to step up the AC voltage to that of the grid. The PV-battery system can be working in either grid-connected or islanded modes by changing the breaker status at the PCC, subject to the condition of the system and the grid, e.g., a serious fault on the AC bus may require opening the breaker to prevent the back-feeding current from the grid [6]. Since PV output power and load demand may change constantly during a day, the power management algorithms for PV-battery system are required to manage the power flow and promptly respond to any change to maintain the balance between power productions and consumptions. Furthermore, both DC bus and AC bus voltages must be stabilized regardless of changes in the system to ensure a reliable power supply.

A number of power management methods for PV-battery systems have been proposed in the literature. An energy management and control system is introduced in [7] which provides stable operation for a wind-PV-battery system. The control algorithm is designed for single-phase inverter and it is not able to control the reactive power. Ref. [8] introduces another control method for a wind-PV-battery system, which focuses on optimizing the sizes and costs of the PV array and battery instead of dynamic power balancing. Moreover, the proposed method requires massive historical data of 30 years to estimate the power generated by the wind turbine and PV array. Similarly, in [9], a method to optimize the wind-PV-battery system is proposed. Both [8] and [9] focus on size optimization instead of detailed control methods for individual power source. A power management strategy for a PV-battery unit is discussed in [10] based on droop control for load sharing between the PV-battery unit and another power source. An improved version, which considers multiple power units, has been presented in Ref. [11]. Although these strategies successfully manage the power demand and production, both of them mainly focus on the power management between the PV-battery unit and other generation units. Additionally, these methods do not consider systems with DC bus and loads. A hierarchical control algorithm for a PV-battery-hydropower

All Rights Reserved © 2018 IJARMATE

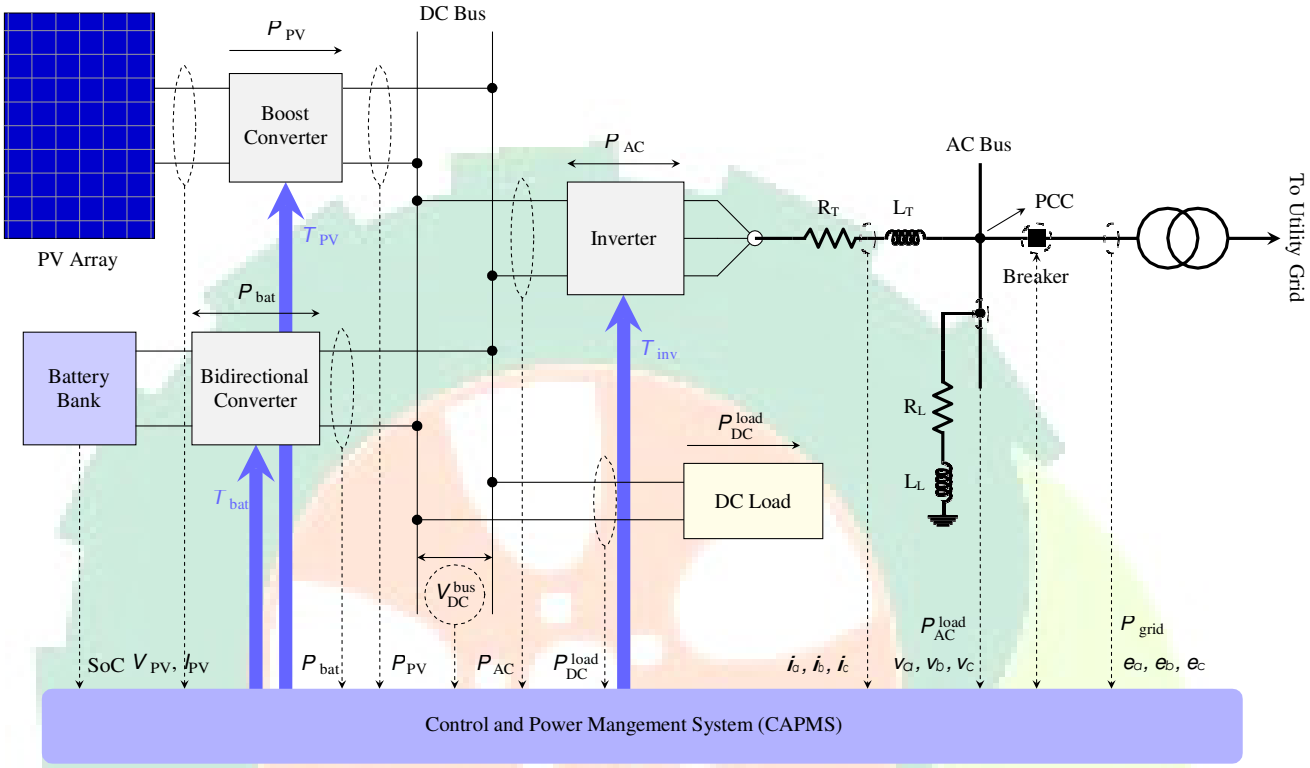

Fig. 1. The proposed control and power management system (CAPMS) for PV-battery-based hybrid microgrids.

system in [12] regulates the AC bus voltage by the hydropower generator and manage the active and reactive power by the PV-battery unit, and Ref. [13] introduces a similar method for a hybrid PV-battery-diesel system. However, both these algorithms fail to consider the voltage control for the case where the hydropower or diesel generator is out of service. A decentralized method for an islanded PV-battery system is presented in [14]. This method aims at solving load sharing in system configurations with multiple PV and battery units. Ref. [15] introduces a similar method which only aims at single-phase low voltage islanded microgrids. None of the aforementioned methods considers the grid-connected situation, where there is power exchange between the hybrid system and the utility grid. Ref. [16] introduces a supervisory control system based on 24-hour forecasted data for a grid-connected wind-PV-battery system. The topology of the studied system, where PV and battery bank are interfaced with the grid using decentralized inverters, is different from the system configuration of this study. Similar methods using day ahead data for power prediction of a PV-battery system are proposed in [17] and [18], which are based on dynamic programming and neural networks, respectively. Ref. [19] proposes a mathematical model for controlling battery storage in PV systems. All these four methods mainly focus on forecasting the power generation and demand, and scheduling the power flow of PV or battery, instead of specific control algorithms. Additionally, there are also works trying to manage the power more effectively by using new topologies of converters [20]–[22] instead of modifying controlling methods. None of the works in the reviewed literature takes into account the stabilization of the DC bus voltage, which is of great importance for reliable power supply for DC loads.

In an attempt to address the issues discussed above, this paper proposes a control and power management system (CAPMS) for PV-battery systems, which is a centralized control system that flexibly and effectively controls power flows among the power sources, loads, and utility grid. The proposed method succeeds in regulating the voltage on both DC and AC buses, transferring between grid-connected and islanded operating modes smoothly, and balancing power quickly in the hybrid PV-battery system. The rest of the paper is organized as follows: Section II and III explain the proposed CAPMS and detailed controllers, after which the proposed method is verified in the case studies of Section IV; Section V concludes the paper.

II. The Proposed Control and Power Management System

Fig. 1 illustrates the configuration of a typical PV-battery system with the proposed CAPMS. In this topology, the PV array is interfaced with the DC bus by a DC/DC boost converter while the battery bank uses a bidirectional DC/DC converter to control the charging and discharging processes. A centralized inverter is installed to interconnect the DC and AC networks. DC load block generally represents the loads that are connecting at the DC bus, which can be multiple types of loads such as electric vehicles or office buildings. There are also AC loads consuming power at the AC bus. This is a typical PV-

All Rights Reserved © 2018 IJARMATE

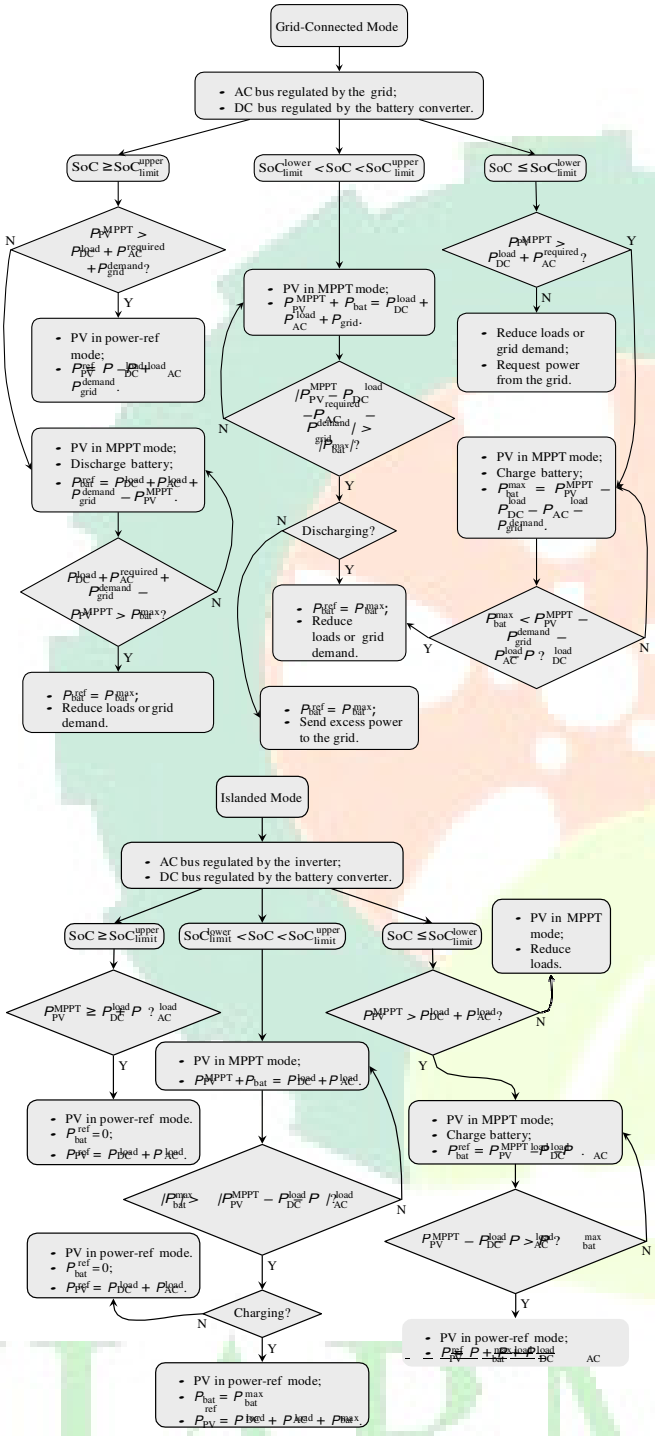

Fig. 2. The power management schemes for grid-connected and islanded modes.

battery microgrid system and similar or same configurations have been widely used and investigated [23]–[26].

The proposed CAPMS is a centralized power management system consisting of a supervisory module that monitors the required real-time parameters (dashed lines in Fig. 1) from the PV-battery system and multiple controllers for each of the power converters. According to the situation of the monitored parameters, CAPMS decides the scenarios and select specific control schemes to be applied to the converters to ensure a reliably power environment. Although the proposed CAPMS is designed based on the PV-battery system configuration shown in Fig. 1, for other configurations, such as systems with decentralized inverters or multiple battery banks, similar approach may be applicable with proper modifications. Detailed schemes of the CAPMS, taking into account both grid-connected and islanded modes, are depicted in Fig. 2, which indicates the possible operating scenarios of the PV-battery microgrid and how CAPMS responds to control and balance the system.

As presented in the flowcharts, the PV-battery system, which connects to the grid via a circuit breaker, can operate either in islanded or grid-connected mode, depending on the conditions and plans of both the microgrid and main grid. Firstly, the CAPMS monitors the status of circuit breaker and determines different voltage and power control schemes to be applied to corresponding converters or inverter. In particular, in grid-connected mode, the inverter controls the DC bus voltage ($V_{\mathrm{DC}}^{\mathrm{bus}}$) and reactive power ($Q_{\mathrm{AC}}$) that is exchanged with the AC side; the PV converter controls the power output of the PV array (P_{PV}); and the battery converter manages the charging or discharging of the battery bank. In islanded mode, where the breaker is open, CAPMS has to ensure the reliability of electric power supplied to the loads, i.e., DC and AC bus voltages and AC frequency have to be maintained around set points within acceptable limits, to prevent damaging the loads during transitions. Therefore, upon transferring from grid-connected to islanded mode, the inverter switches to regulate the AC bus voltage (v_a, v_b, and v_c) and frequency (f), while $V_{\mathrm{DC}}^{\mathrm{bus}}$ is regulated by the battery converter. Secondly, state of charge (SoC) of the battery bank is always monitored in both modes. Therefore, CAPMS is aware of the available energy storage that can be used in the battery. The upper and lower limits of the SoC ($\mathrm{SoC}_{\mathrm{limit}}^{\mathrm{upper}}$ and $\mathrm{SoC}_{\mathrm{limit}}^{\mathrm{lower}}$) are set up to make sure the battery is not over-charged or discharged and to increase its cycle life [27]. Depending on the PV output power, SoC and power limit of the battery, DC and AC loads, and the grid demand, CAPMS decides the operation modes of the PV array (MPPT or power-reference mode) and the battery (charging or discharge mode) and provides proper reference values to the controllers, if applicable. Therefore, power flows in the hybrid microgrid are always balanced. The power management criteria are based on

$$\text{Grid-connected}: P_{\mathrm{PV}} + P_{\mathrm{bat}} = P_{\mathrm{DC}}^{\mathrm{load}} + P_{\mathrm{AC}}^{\mathrm{load}} + P_{\mathrm{grid}}, \quad (1)$$

$$\text{Islanded}: P_{\mathrm{PV}} + P_{\mathrm{bat}} = P_{\mathrm{DC}}^{\mathrm{load}} + P_{\mathrm{AC}}^{\mathrm{load}}, \quad (2)$$

where P_{PV} is the output power of the PV array, P_{bat} is the power flows in the battery converter ($P_{\mathrm{bat}} < 0$ in charging mode and $P_{\mathrm{bat}} > 0$ in discharging mode), $P_{\mathrm{DC}}^{\mathrm{load}}$ and $P_{\mathrm{AC}}^{\mathrm{load}}$ are DC and AC loads, respectively, and P_{grid} generally represents the power exchanging between the main grid and the microgrid through the breaker ($P_{\mathrm{grid}} < 0$ when receiving power and $P_{\mathrm{grid}} > 0$ when sending power). Note that the power demand

All Rights Reserved © 2018 IJARMATE

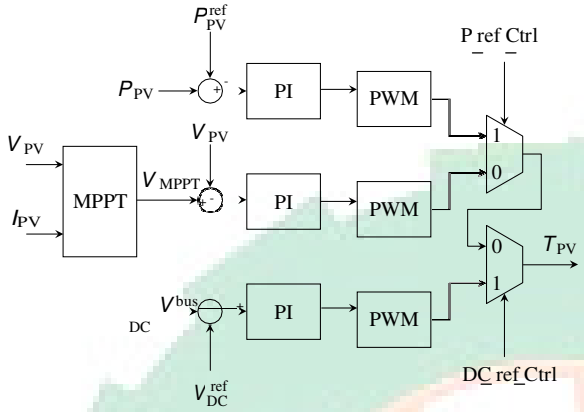

Fig. 3. PV array controller.

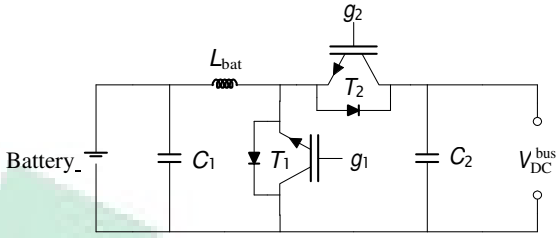

Fig. 4. Bidirectional DC/DC converter for the battery bank.

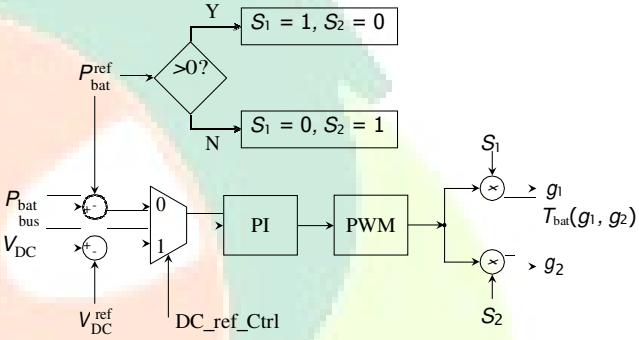

Fig. 5. Battery charging/discharging controller.

from the main grid is denoted as P^{demand}_{grid} (Fig. 2), which might be obtained by forecasting data. Before switching from islanded to grid-connected mode, CAPMS will synchronize the AC voltages at the PCC of the microgrid to follow the grid-side voltages to ensure a smooth transition.

With well-balanced power and regulated voltages, CAPMS ensures an uninterrupted power on both DC and AC buses and allows loads to plug and play in the PV-battery system, regardless of disturbances from switching operating modes. Additionally, since the DC bus voltage is controlled, as long as voltage level matches, DC loads will be able to connect to the DC bus without additional converters. When necessary, the PV-battery system can also provide reactive power to the grid. Detailed controlling schemes for each part of the system will be elaborated in the next section.

III. Controller Design of The CAPMS

A. PV Array Controller

The PV array converts solar energy into DC power, and is connected to the DC bus via a boost DC/DC converter. However, due to nonlinear characteristics of PV panels and the stochastic fluctuations of solar irradiance, there is always a maximum power point (MPP) for every specific operating situation of a PV array. Therefore, maximum power point tracking (MPPT) algorithms are typically implemented in PV system to extract the maximum power a PV array can provide [28]. The proposed CAPMS employs one of the most popular methods, the Incremental Conductance MPPT, which provides a reference voltage V_{MPPT} that the PV array will track to produce the maximum power under various operation conditions (different combinations of irradiance and temperature). There are three possible control schemes for the PV array: MPPT control, power-reference control, and DC bus voltage control, depending on the situation of the PV-battery system. For example, in islanded mode, when P^{MPPT}_{PV} is greater than the total load demand (DC and AC), and the battery is fully charged or the charging rate P_{bat} reaches its upper limit, the CAPMS will generate control commands P_ref_Ctrl = 1 and DC_ref_Ctrl = 0 to set the PV array to work in power-reference control mode by sending PWM streams, T_{PV}, to the DC/DC converter accordingly. In this case, to balance the power flows, CAPMS will decide proper power references for the PV array, P^{ref}_{PV}, according to the value of which the operating voltage of the PV array, V_{PV}, will be moving between its V_{MPPT} and the open-circuit voltage, V_{OC}. Since the DC bus voltage is regulated by the battery converter in this situation, there will be a stable voltage at the DC bus in spite of the fluctuations in V_{PV}. In MPPT mode (P_ref_Ctrl = 0 and DC_ref_Ctrl = 0), real-time PV current, I_{PV}, and V_{PV} are measured and sent to the MPPT module, which then provides V_{MPPT} as the voltage reference for the PV array. Additionally, in islanded mode, when the battery is not available, e.g., due to faults, the PV converter has to switch to control the DC bus voltage to ensure a stable power supply to the loads on the DC bus (P_ref_Ctrl = 0 and DC_ref_Ctrl = 1). Fig. 3 illustrates the controller for these three modes. Note that the situation where both P_ref_Ctrl = 1 and DC_ref_Ctrl = 1 is not applicable.

B. Battery Controller

As an energy buffer, battery bank is necessary in PV systems for power balancing. The battery bank of this system is connected to the DC bus and is controlled by a bidirectional DC/DC converter (Fig. 4) which includes two switches, T_1 and T_2, that control the charging/discharging process. Fig. 5 explains the detailed control process. In grid-connected mode, with the command DC_ref_Ctrl = 0, the converter controls the power flow (P_{bat}) in or out of the battery, where in discharging mode $P_{bat} > 0$, and in charging mode $P_{bat} < 0$. The final output of the battery controller is a two-dimensional switching signal $T_{bat}(g_1, g_2)$. In Islanded mode, the control command DC_ref_Ctrl is set to "1" by the CAPMS, which switches

All Rights Reserved © 2018 IJARMATE

the converter to work in voltage reference mode. The output voltage of converter, which is also the DC bus voltage, is regulated to follow the reference so that the DC load voltage is stabilized. The CAPMS monitors the SoC of the battery and enforces its upper and lower limits (SoC^{upper}_{limit} = 90% and SoC^{lower}_{limit} = 10% in this study) in order to increase the life cycle. Note that the selections of the SoC limits do not affect the performance of the controller.

C. Inverter Controller

A three-phase inverter is used to convert DC to AC power, interfacing the DC and AC sides. Similar to the converters discussed above, the control scheme of inverter depends on the operating (grid-connected or islanded) mode of the system. As is illustrated in Fig. 1 and 6, in grid-connected mode, a phase-locked loop (PLL block) is employed to extract θ, angle the of phase-A voltage after the breaker(e_a). In islanded mode, θ is generated locally, which is periodical ramp signal varying from 0 to 2π with frequency f. It is used to decompose the three-phase AC bus voltages (v_a, v_b and v_c) and the inverter output currents (i_a, i_b and i_c) into d-q frame variables V_d and V_q, and I_d and I_q by Park transformation, respectively, for control purposes. Depending on the operating mode, the controller selects different sets of variables to be controlled. Under islanded mode, CAPMS sets the signal "Islanded" to 1, forcing the converter to regulate the AC bus voltage V_d and V_q. Frequency of the AC bus voltages (f) is set to 60 Hz in a open-loop manner. Before closing the breaker and reconnecting the PV-battery system to the grid, the AC bus voltage must be synchronized with the grid. During islanded mode, the signal "Sync" is set to 0 so that CAPMS has full control of the AC bus voltage by adjusting the references, V^{ref}_d and V^{ref}_q. However, to ensure a smooth transition upon switching to grid-connected mode, "Sync" will be set to 1 to synchronize the AC bus and grid side voltages right before closing the breaker. To this end, θ will be synchronized to follow the output angle of PLL, and the AC voltages after the breaker in d-q frame, E_d and E_q, will be chosen as the references for V_d and V_q (Fig. 6), respectively. In grid-connected mode (Islanded = 0), the inverter is responsible for regulating the DC bus voltage V_{DC} and controlling the reactive power transferring from DC to AC side. Additionally, in both operating modes, the current references of inner loop of the controller (I^{ref}_d and I^{ref}_q) can be enforced to proper limits to prevent overloading of the inverter.

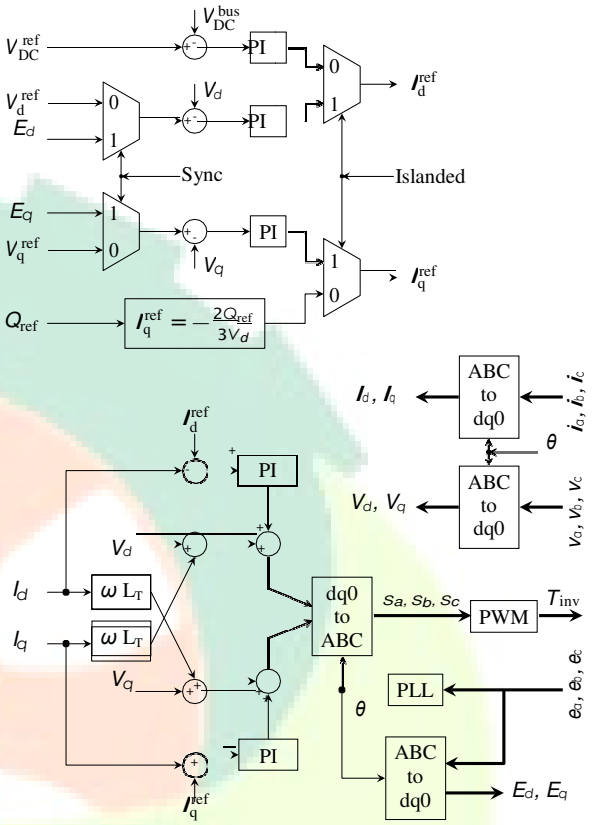

Fig. 6. Control scheme of the inverter.

TABLE I
BASIC PARAMETERS OF THE PV-BATTERY SYSTEM UNDER STC

Parameters	Values
PV Maximum Power (P_{PV}^{MPPT})	170 kW
PV Maximum Power Voltage (V_{MPPT})	122 V
Battery Capacity	45 kAh
Battery Fully Charged Voltage	412.5 V
Battery Nominal Voltage	400 V
Battery Max Charge/Discharge Power	150 kW
DC Bus Voltage (V_{DC}^{ref})	450 V
AC Bus Voltage (line to line)	208 V
Transformer Voltage Ratio	208 V : 1.2 kV

IV. CASE STUDIES

In order to verify the performance of the proposed CAPMS, numerous simulation and experimental case studies are carried out in this section using the PSCAD/EMTDC and Matlab/Simulink software package and the dPACE-DS1104 platform. A PV-battery system is constructed with the configuration presented in Fig. 1, with the parameters listed in Table I. Note that the parameters for the PV array are under standard testing condition (STC, irradiance = 1000 W/m^2, temperature = 25°C). The battery bank uses a general Ni-Cd characteristic model whose capacity is sized according to the IEEE Standard 1562-2007 [29] to support 5 days of autonomy operation (for 150 kW loads) under low irradiance conditions. The proposed CAPMS monitors the required variables out of the PV-battery system mentioned in the above sections, process the data following the schemes in Fig. 2, and, according to the situation observed, switches the control schemes automatically. The case studies test the CAPMS's responses for multiple scenarios that the PV-battery system is working in or switching to. Results are analyzed individually in each case.

A. Simulation Verification: Grid-Connected Mode

1) Case A-1: The first case is the normal operation situation of the PV-battery system in grid-connected mode, when the battery is fully available for power balancing (10% < SoC < 90%). PV array is working in MPPT mode, tracking the

All Rights Reserved © 2018 IJARMATE

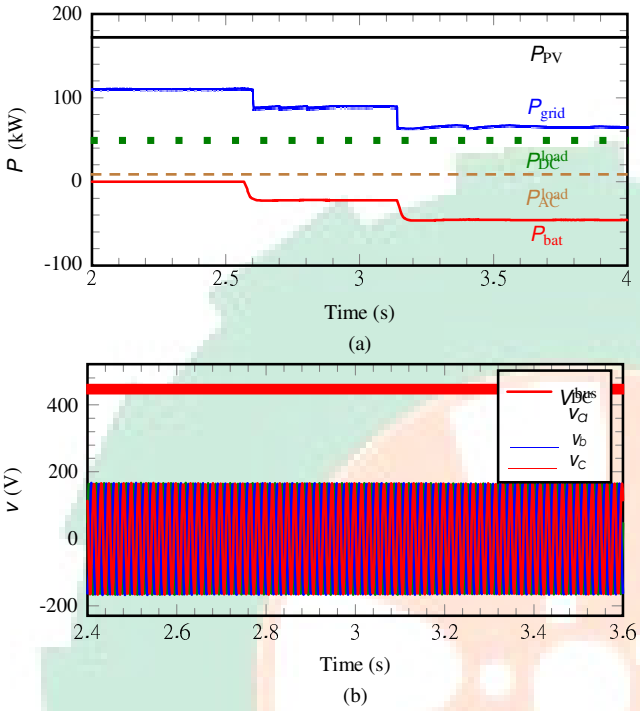

Fig. 7. Grid-connected mode Case A-1: (a) power flows and (b) voltage values of the PV-battery system.

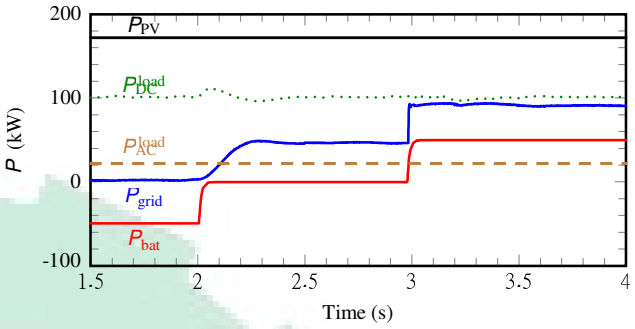

Fig. 8. Grid-connected mode Case A-2: power flows of the PV-battery system.

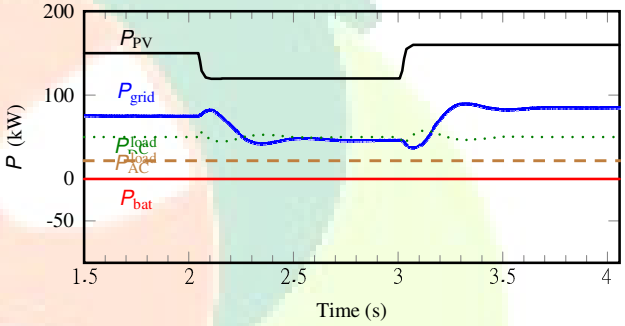

Fig. 9. Grid-connected mode Case A-3-1: PV array in power-reference mode.

voltage reference (V_{MPPT}) estimated by the MPPT module. DC and AC loads are supplied by the buses. Depending on the amount of generation, load, and demand requested by the grid (P_{grid}), the battery is balancing the power by absorbing or releasing power. Fig. 7 presents the power flows and voltages of the PV-battery system under the control of CAPMS in Case A-1. Before 2.6 s, the PV array power P_{PV} is around 170 kW in MPPT mode, which is shared by the DC load (P_{DC}^{load} = 50 kW), AC load (P_{AC}^{load} = 10 kW), and the utility grid (P_{grid} = −110 kW). The power flow in or out of the battery during this period is about 0 since no extra power is available. At about 2.6 s, as the grid demand decreases to around 85 kW, 15 kW extra power is sent to charge the battery (P_{bat} = 15 kW). Later at 3.15 s, the grid demand drops again, and the battery power continues to increase. As long as the battery SoC and P_{bat} are within the limits, the battery is able to balance the power as an energy buffer. During these changes, the DC and AC bus voltages are controlled (Fig. 7).

2) Case A-2: As the battery is charged, the SoC will keep increasing. When the battery SoC is greater than 90 %, CAPMS will stop charging the battery and send the surplus power to the grid. Whenever the demand increases, the energy stored in the battery will be released to complement the change. Fig. 8 illustrates these processes. At 2 s, the battery is fully charged and the CAPMS sets P_{bat}^{ref} to 0. Thereby, P_{bat} follows the reference and the excess power of the system is delivered to the grid (P_{grid} increases to 50 kW at 2 s). At 3 s, the demand from grid (P_{grid}^{demand}) increases to about 95 kW. Since the PV array is working in MPPT mode (P_{PV} = 170 kW), and the DC and AC loads require 125 kW totally (P_{DC}^{Load} = 103 kW and P_{AC}^{Load} = 22 kW), the battery has to be controlled to provide 50 kW to balance the power.

3) Case A-3: There is also situation where the SoC of battery has reached the upper limits (90 %), however, the maximum power provided by the PV array is more than the demands and loads. In this case, since the battery has been fully charged, and if the grid cannot absorb the excess power from PV array, CAPMS will switch the operating mode of PV from MPPT to power-reference mode to balance the system, as is presented in Fig. 9 (Case A-3-1). Before 2 s, P_{PV} is set to 150 kW, and P_{bat} is set to 0. Therefore, besides the DC and AC load, (50 and 25 kW, respectively), excess power is sent to the grid (P_{grid} = 75 kW). As the reference of PV power changes at 2 s and 3 s, the power sent to grid adapts accordingly, keeping the power balanced in the PV-battery system. Fig. 10 (Case A-3-2) shows the smooth changes of PV voltage (blue curve) and the stable DC bus voltage (red curve) during the transitions between MPPT and power-reference modes. Note that V_{PV} is greater than V_{MPPT} but less than V_{OC} in power-reference mode, and the PV operating point depends on the value of P_{PV}^{ref}.

4) Case A-4: The power flow in the inverter is bidirectional, i.e., when necessary, the PV-battery system can request power from the grid. For instance, when there is available power from the grid and the PV-battery system has more demand than generation, the CAPMS can reverse the power through the inverter to supply the system. Fig.11 gives an example of this situation. The battery SoC is less than 10% which hits the lower limit and stops releasing power for battery protection. The PV array is supplying power to the DC and AC loads

All Rights Reserved © 2018 IJARMATE

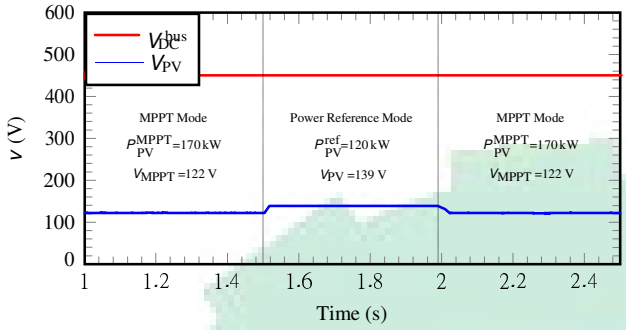

Fig. 10. Grid-connected mode Case A-3-2: DC bus and PV array voltages during transitions between MPPT and power-reference modes.

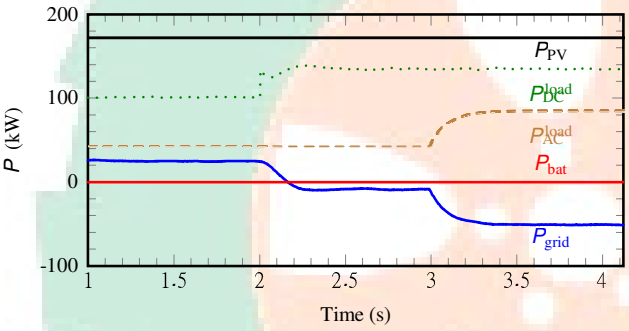

Fig. 11. Grid-connected mode Case A-4: the PV-battery system is receiving power from the grid after 2.2 s.

and the grid. However, DC load increases suddenly at 2 s, which causes the DC system to request power from the grid. Hence, P_{grid} becomes negative, delivering reversed power in the inverter from the grid to the DC load. Immediately after that, at 3 s, the AC load increases. Since the battery bank is still not available, power from the grid increases to balance the system. Case study A-4 shows the proposed CAPMS rapidly responds to this situation.

5) Case A-5: In grid-connected mode, since the inverter has full control of the DC bus voltage as well as the reactive power, it is able to provide reactive power to the grid if necessary. The waveforms associated with this case are plotted in Fig. 12, where the blue and red curves are the active and reactive power, P_{grid} and Q_{grid}, respectively, that are being transferred from the PV-battery system to the grid. The inverter controls the reactive power flexibly. Regardless of changes of Q_{grid}, P_{grid} is stabilized at its value.

6) Case A-6: As is mentioned in previous sections, the PV-battery system may work in either grid-connected or islanded modes. For example, when the utility grid is unstable or there are severe faults at the AC bus, to prevent drawing back-feeding current from the grid, the circuit breaker at PCC will open, switching the system to work in islanded mode. After operating the breaker, the inverter is switched to control the AC bus voltage and frequency (Fig. 6), while the DC bus voltage is controlled by the battery converter (Fig. 5). Fig. 13 presents the dynamics of the DC and AC bus voltages (operating mode is changed at 1.4 s), where the voltages take less than 0.05 s

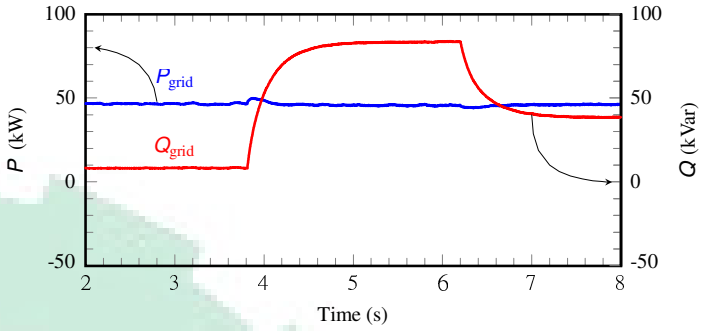

Fig. 12. Grid-connected mode Case A-5: Reactive power control of the inverter.

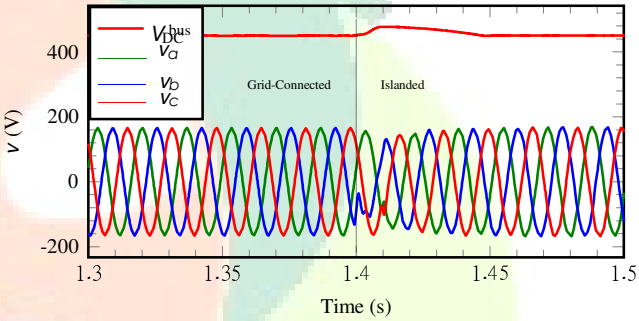

Fig. 13. Grid-connected mode Case A-6: transition from grid-connected to islanded mode.

to settle.

B. Simulation Verification: Islanded Mode

1) Case B-1: When the PV-battery system works in islanded mode, the available power is provided by PV or battery only, and the power balance criterion follows equation $P_{PV} + P_{bat} = P_{DC}^{load} + P_{AC}^{load}$. Under normal operation conditions, where the battery SoC is within the lower (10%) and upper (90%) limits, PV array tracks V_{MPPT} provided by the MPPT module and provides power to the DC and AC loads. Power going through the battery converter might be in either direction, depending on the load demand and PV output. Fig. 14 shows an example of power sharing between PV and the battery bank: a 20 kW increase of AC bus load (P_{AC}^{load}) at 1.2 s results in a decrease of battery charging power (P_{bat}) from 50 kW to 30 kW; and another precipitous increase of DC load at 2.5 s poses the battery to discharge power in order to fulfill the system demand. It is verified in this case that the proposed CAPMS successfully responds to manage these changes.

2) Case B-2: Solar irradiance may change in seconds, resulting in PV power oscillations that will influence the load in both DC and AC buses. With the help of battery bank and the proposed CAPMS, the change of PV power can be compensated effectively by adapting the power flow in the battery converter. Fig. 15 shows how the battery power (red solid curve) responds to the decline of PV power due to reducing solar irradiance. Case study B-2 proves that CAPMS is capable of controlling the battery to balance the power quickly and precisely.

All Rights Reserved © 2018 IJARMATE

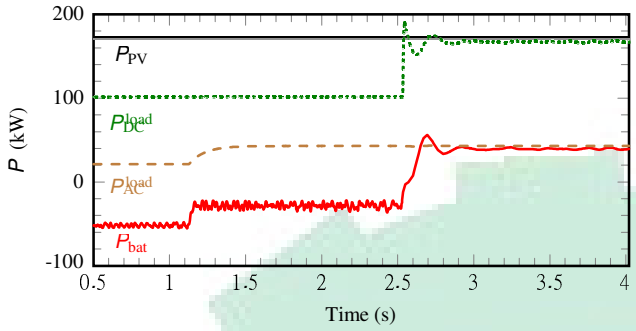

Fig. 14. Islanded mode Case B-1: power flows of the PV-battery system with changing loads.

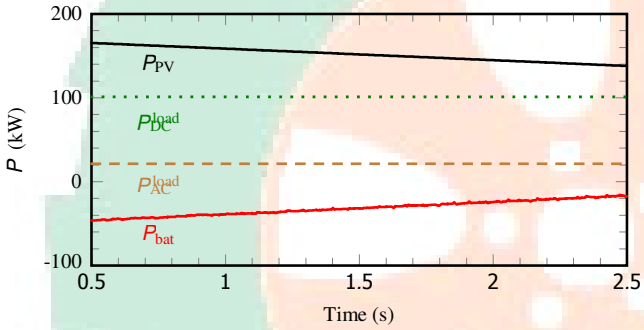

Fig. 15. Islanded mode Case B-2: battery power changes with PV generation.

3) Case B-3: Unlike grid-connected mode, V_{DC}^{bus} and AC bus voltages (v_a, v_b and v_c) are controlled by the battery converter and inverter, respectively. Normally, bus voltages have to be regulated at certain values in order to provide reliable power to loads. Nevertheless, the CAPMS also has full control of these voltages. Both DC and AC bus voltages can be scaled by changing their references (Fig. 5 and 6). A case study of changing the DC (at 1 s) and AC bus voltages (at 1.55 s and 1.97 s) is presented in Fig. 16.

4) Case B-4: Disconnecting the PV-battery system might result from accidental actions of the breaker at the PCC. However, reconnecting the system to grid is usually pre-planned, i.e., before closing the breaker, the operator will have sufficient time to posture the standalone PV-battery system for a smooth reconnection. One of the most important parameters to control is the three-phase AC bus voltage, which has to be synchronized with the voltage at the grid side PCC to avoid disturbances introduced by the action of breaker. This case compares the situations where the AC bus voltage is synchronized by the CAPMS, and is not synchronized before closing the breaker. In Fig. 17 (a), waveform distortion can be observed at the inception of closing the breaker (at 1.025 s) without voltage synchronization. In contrast, Fig. 17 (b) presents the synchronizing process, which takes only approximately one cycle but successfully avoids the distortion. This greatly reduces the disturbances, ensuring a stable power supply to the loads on the AC bus when reconnecting the PV-battery system to the grid.

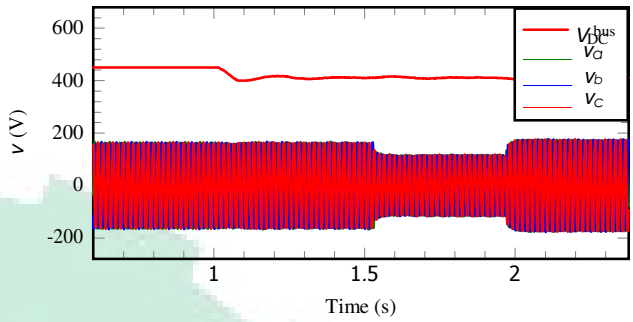

Fig. 16. Islanded mode Case B-3: bus voltage control of the PV-battery system.

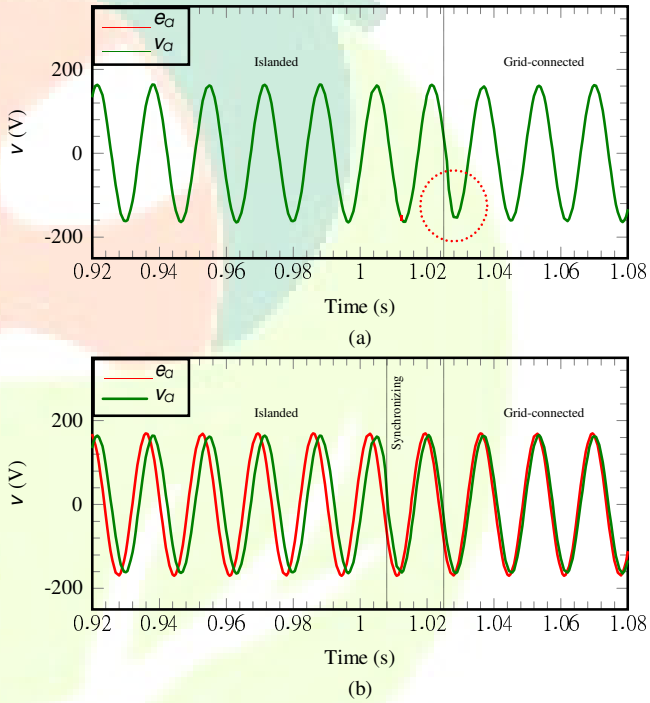

Fig. 17. Islanded mode Case B-4: (a) unsynchronized and (b) synchronized AC bus voltages (displaying phase-a) when closing the breaker at the PCC.

C. Experimental Verification

To further verify the performance of the CAPMS, experimental case studies are carried out and presented in this subsection. An islanded PV-battery hybrid system is built using the same configuration illustrated in Fig. 1. dSPACE-DS1104 workstation is employed to interface the microgrid and the CAPMS that is implemented in the Matlab/Simulink software package. Fig. 18 shows the experimental setups. The PV panel and the lead-acid battery are interfacing the DC bus using two DC/DC converters, which control the PV power and the charging/discharging of battery, respectively. A 100 Ω DC load is added to the DC bus. An inverter is used to convert DC to AC power and the three-phase AC loads are connected at the output of the inverter. Table II lists the specifications for the experimental PV panel and the battery under STC. The voltage, current, and power of each unit and the SoC

All Rights Reserved © 2018 IJARMATE

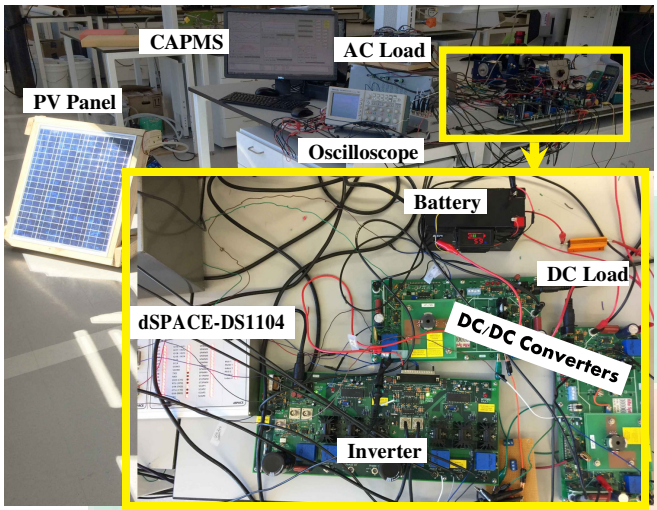

Fig. 18. Experimental PV-battery hybrid microgrid.

TABLE II
SPECIFICATIONS OF THE PV PANEL AND BATTERY UNDER STC

Device	Parameter
PV Panel	I_{SC}^{STC} = 3.1 A, V^{STC} = 19.3 V, V_{MPPT}^{STC} = 17.5 V, P_{MPPT}^{STC} = 59.83 W.
Battery	Capacity = 7 Ah, Nominal Voltage = 12 V, Max Charging/Discharging Current = 2 A.

of the battery are monitored by dSPACE. According to the status of the aforementioned parameters, CAPMS optimizes the reference values for each unit and sends the PWM signals to the inverter and converters to control the power flows in the hybrid system and voltages of the DC and AC buses. In the experimental setup, the DC bus voltage is controlled at 32 V, and the AC bus voltage is converted to the dq-frame and is controlled such that $V_d = 7$ V and $V_q = 0$ V.

1) Case C-1: As is presented in Section II and III, in islanded mode, the DC bus voltage is regulated by the battery converter, while the inverter controls the AC bus voltage and frequency. In practice, the voltage of a PV array depends on the irradiance it receives. Especially, the PV voltage may fluctuate significantly during cloudy days due to unstable irradiance, or a short-circuit fault may result in zero PV voltage. Experiments show that, the CAPMS is able to stabilize the bus voltages despite these disturbances. Fig. 19 presents the screen capture of the oscilloscope which monitors the voltages of the battery (V_{bat}, CH1), PV panel (V_{PV}, CH2), DC bus (V_{bus}^{DC}, CH3) and the AC d-frame (V_d, CH4). In the experiment, V_{PV} is reduced manually from approximately 17 V to 5 V and then to zero (blue curve in Fig. 19). However, the DC and AC bus voltages (green and purple curves, respectively) are regulated by the CAPMS and keep tracking their reference values. A change of the DC bus voltage (V_{bus}^{DC}) also does not affect the other voltages. As is presented in Fig. 20, V_{bus}^{DC} is increased from 32 V to near 40 V (green curve), while the other voltages are not affected.

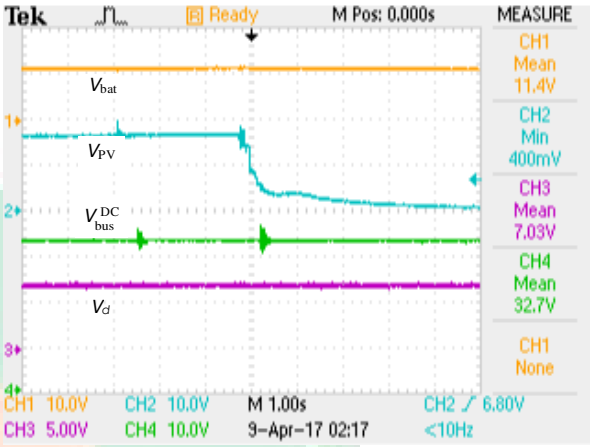

Fig. 19. Experiment Case C-1: oscilloscope screen capture for the change of PV panel voltage.

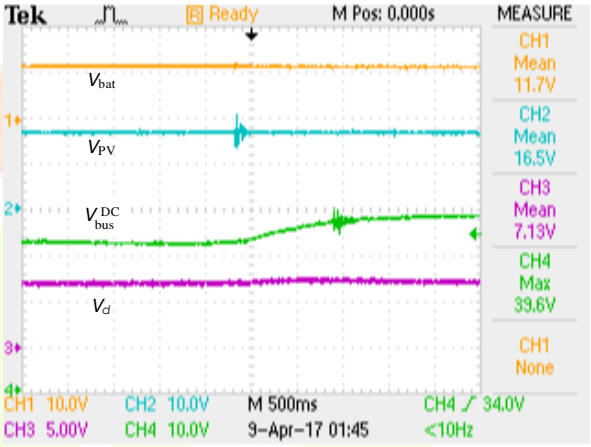

Fig. 20. Experiment Case C-1: oscilloscope screen capture for the change of DC bus voltage.

2) Case C-2: In islanded mode, the CAPMS balances the power flows in the PV-battery hybrid microgrid such that power generation matches the load demand ($P_{PV} + P_{bat} = P_{DC}^{load} + P_{AC}^{load}$). When the PV power fluctuates because of an unstable irradiance, the battery will respond to ensure a reliable power to the DC and AC loads. In a worse situation, the PV panel may shut down due to insufficient irradiance or faults. The battery should be able to support the entire microgrid until the PV power resumes. In the experiments, the irradiance received by the PV panel in the laboratory is less than 1000 W/m^2, which leads P_{MPPT} to be around 16 W. A 10.24 W and a three-phase 4.2 W load are added to the DC and AC buses, respectively. The system power losses is approximately 3.5 W. Fig. 21 presents the power of each unit captured by the dSPACE. From 0 to 5 s, the PV panel is providing it maximum power P_{PV} = 16 W (black curve) while the battery is providing 2 W (red curve) to the system. At 5 s, the angle of the PV panel is moved such that the PV power is reduced. The battery responds rapidly by increasing its power to compensate this change. At 15 s, the PV converter is shut down and the PV power reduces to zero. The battery

All Rights Reserved © 2018 IJARMATE

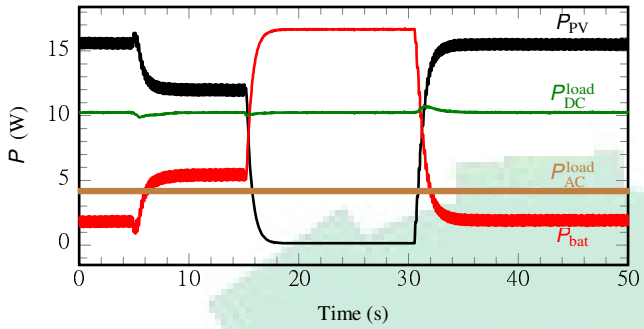

Fig. 21. Experiment Case C-2: dSPACE captures of the power of each unit.

power increases immediately to support the entire system. At 30 s, the PV power resumes to its maximum power point, and the battery power decreases accordingly. It is noteworthy that during these transitions, the DC and AC bus power are successfully stabilized (green and brown curves). The CAPMS succeeds in balancing the power flows in the PV-battery hybrid system and providing reliable power to the loads on both the DC and AC buses.

V. Conclusions

This paper proposes a control and power management system (CAPMS) for hybrid PV-battery systems with both DC and AC buses and loads, in both grid-connected and islanded modes. The presented CAPMS is able to manage the power flows in the converters of all units flexibly and effectively, and ultimately to realize the power balance between the hybrid microgrid system and the grid. Furthermore, CAPMS ensures a reliable power supply to the system when PV power fluctuates due to unstable irradiance or when the PV array is shut down due to faults. DC and AC buses are under full control by the CAPMS in both grid-connected and islanded modes, providing a stable voltage environment for electrical loads even during transitions between these two modes. This also allows additional loads to access the system without extra converters, reducing operation and control costs. Numerous simulation and experimental case studies are carried out in Section IV that verifies the satisfactory performance of the proposed CAPMS.

References

[1] T. A. Nguyen, X. Qiu, J. D. G. II, M. L. Crow, and A. C. Elmore, "Performance characterization for photovoltaic-vanadium redox battery microgrid systems," *IEEE Trans. Sustain. Energy*, vol. 5, no. 4, pp. 1379–1388, Oct 2014.

[2] S. Kolesnik and A. Kuperman, "On the equivalence of major variable-step-size MPPT algorithms," *IEEE J. Photovolt.*, vol. 6, no. 2, pp. 590–594, March 2016.

[3] H. A. Sher, A. F. Murtaza, A. Noman, K. E. Addoweesh, K. Al-Haddad, and M. Chiaberge, "A new sensorless hybrid MPPT algorithm based on fractional short-circuit current measurement and P&O MPPT," *IEEE Trans. Sustain. Energy*, vol. 6, no. 4, pp. 1426–1434, Oct 2015.

[4] Y. Riffonneau, S. Bacha, F. Barruel, and S. Ploix, "Optimal power flow management for grid connected PV systems with batteries," *IEEE Trans. Sustain. Energy*, vol. 2, no. 3, pp. 309–320, July 2011.

[5] H. Kim, B. Parkhideh, T. D. Bongers, and H. Gao, "Reconfigurable solar converter: A single-stage power conversion PV-battery system," *IEEE Trans. Power Electron.*, vol. 28, no. 8, pp. 3788–3797, Aug 2013.

[6] Z. Yi and A. H. Etemadi, "A novel detection algorithm for line-to-line faults in photovoltaic (PV) arrays based on support vector machine (SVM)," in *2016 IEEE Power and Energy Society General Meeting (PESGM)*, July 2016, pp. 1–4.

[7] A. Merabet, K. Ahmed, H. Ibrahim, R. Beguenane, and A. Ghias, "Energy management and control system for laboratory scale microgrid based wind-PV-battery," *IEEE Trans. Sustain. Energy*, vol. PP, no. 99, pp. 1–1, 2016.

[8] B. S. Borowy and Z. M. Salameh, "Methodology for optimally sizing the combination of a battery bank and PV array in a wind/PV hybrid system," *IEEE Trans. Energy Convers.*, vol. 11, no. 2, pp. 367–375, Jun 1996.

[9] D. Abbes, A. Martinez, and G. Champenois, "Eco-design optimisation of an autonomous hybrid wind-photovoltaic system with battery storage," *IET Renewable Power Generation*, vol. 6, no. 5, pp. 358–371, Sept 2012.

[10] H. Mahmood, D. Michaelson, and J. Jiang, "A power management strategy for PV/battery hybrid systems in islanded microgrids," *IEEE J. Emerg. Sel. Top. Power Electron*, vol. 2, no. 4, pp. 870–882, Dec 2014.

[11] H. Mahmood, D. Michaelson and J. Jiang, "Decentralized power management of a PV/battery hybrid unit in a droop-controlled islanded microgrid," *IEEE Trans. Power Electron.*, vol. 30, no. 12, pp. 7215–7229, Dec 2015.

[12] Y. Guan, J. C. Vasquez, J. M. Guerrero, Y. Wang, and W. Feng, "Frequency stability of hierarchically controlled hybrid photovoltaic-battery-hydropower microgrids," *IEEE Trans. Ind. Appl.*, vol. 51, no. 6, pp. 4729–4742, Nov 2015.

[13] J. Philip, C. Jain, K. Kant, B. Singh, S. Mishra, A. Chandra, and K. Al-Haddad, "Control and implementation of a standalone solar photovoltaic hybrid system," *IEEE Trans. Ind. Appl.*, vol. 52, no. 4, pp. 3472–3479, July 2016.

[14] Y. Karimi, H. Oraee, M. Golsorkhi, and J. Guerrero, "Decentralized method for load sharing and power management in a PV/battery hybrid source islanded microgrid," *IEEE Trans. Power Electron.*, vol. PP, no. 99, pp. 1–1, 2016.

[15] M. S. Golsorkhi, Q. Shafiee, D. Lu, and J. M. Guerrero, "A distributed control framework for integrated photovoltaic-battery based islanded microgrids," *IEEE Trans. Smart Grid*, vol. PP, no. 99, pp. 1–1, 2016.

[16] A. C. Luna, N. L. D. Aldana, M. Graells, J. C. Vasquez, and J. M. Guerrero, "Mixed-integer-linear-programming based energy management system for hybrid PV-wind-battery microgrids: Modeling, design and experimental verification," *IEEE Trans. Power Electron.*, vol. PP, no. 99, pp. 1–1, 2016.

[17] Y. Riffonneau, S. Bacha, F. Barruel, and S. Ploix, "Optimal power flow management for grid connected PV systems with batteries," *IEEE Trans. Sustain. Energy*, vol. 2, no. 3, pp. 309–320, July 2011.

[18] M. Brenna, F. Foiadelli, M. Longo, and D. Zaninelli, "Energy storage control for dispatching photovoltaic power," *IEEE Trans. Smart Grid*, vol. PP, no. 99, pp. 1–1, 2016.

[19] J. H. Teng, S. W. Luan, D. J. Lee, and Y. Q. Huang, "Optimal charging/discharging scheduling of battery storage systems for distribution systems interconnected with sizeable PV generation systems," *IEEE Trans. Power Syst.*, vol. 28, no. 2, pp. 1425–1433, May 2013.

[20] S. Mishra, D. Pullaguram, S. A. Buragappu, and D. Ramasubramanian, "Single-phase synchronverter for a grid-connected roof top photovoltaic system," *IET Renewable Power Generation*, vol. 10, no. 8, pp. 1187–1194, 2016.

[21] F. Nejabatkhah, S. Danyali, S. H. Hosseini, M. Sabahi, and S. M. Niapour, "Modeling and control of a new three-input DC-DC boost converter for hybrid PV/FC/battery power system," *IEEE Trans. Power Electron.*, vol. 27, no. 5, pp. 2309–2324, May 2012.

[22] H. Zhu, D. Zhang, B. Zhang, and Z. Zhou, "A nonisolated three-port DC-DC converter and three-domain control method for PV-battery power systems," *IEEE Trans. Ind. Electron.*, vol. 62, no. 8, pp. 4937–4947, Aug 2015.

[23] L. Xu, X. Ruan, C. Mao, B. Zhang, and Y. Luo, "An improved optimal sizing method for wind-solar-battery hybrid power system," *IEEE Trans. Sustain. Energy*, vol. 4, no. 3, pp. 774–785, July 2013.

[24] M. O. Badawy and Y. Sozer, "Power flow management of a grid tied pv-battery system for charging of electric vehicles," *IEEE Trans. Ind. Appl.*, vol. PP, no. 99, pp. 1–1, 2016.

[25] A. Merabet, K. T. Ahmed, H. Ibrahim, R. Beguenane, and A. M. Y. M. Ghias, "Energy management and control system for laboratory scale microgrid based wind-pv-battery," *IEEE Trans. Sustain. Energy*, vol. 8, no. 1, pp. 145–154, Jan 2017.

All Rights Reserved © 2018 IJARMATE

IJARMATE
Fourth MATE Research Paper